Adsorption (2007) 13: 173–189
DOI 10.1007/s10450-007-9033-5

Water adsorption with hysteresis effect onto microporous activated carbon fabrics

Patrick D. Sullivan · Brenton R. Stone · Zaher Hashisho · Mark J. Rood

Received: 30 April 2007 / Revised: 30 April 2007 / Accepted: 23 July 2007 / Published online: 28 September 2007
© Springer Science+Business Media, LLC 2007

Abstract Understanding the adsorption of water vapor onto activated carbons is important for designing processes to remove dilute contaminants from humid gas streams, such as providing protection against chemical warfare agents (CWAs), or against toxic industrial compounds (TICs) used in a terrorist chemical attack. Water vapor isotherms for Calgon BPL granular activated carbon (GAC), military ASZM-TEDA GAC, electrospun activated carbon nanofibers (ACnF), Calgon Zorflex™ activated carbon cloth, and Novoloid-based activated carbon fiber cloth (ACFC) are presented. Of particular interest are the ACFC isotherms, which exhibit an unusually high degree of hydrophobicity. The ACFC isotherms also show a correlation between water vapor adsorption hysteresis and the level of activation. Water vapor isotherm models from the literature are compared.

Keywords Activated Carbon Fiber Cloth (ACFC) · Water vapor adsorption · Hysteresis · Isotherm models

Abbreviations

A	Distribution constant for Mahle equation
a	Amount adsorbed at a given p_r
a_c	Constant for DS4 equation
a_f	Capacity of functional site part of Do & Do type equations
a_I	Capacity of type I term of Stoeckli formula, or capacity of Ising term in Extended CMMS equation
a_L	Capacity of Langmuir term of Extended CMMS formula
a_m	Capacity constant in Talu–Meunier equation
a_o	Pore capacity
a_p	Concentration of primary sites
a_V	Capacity of type V term in Stoeckli equation
a_μ	Capacity of microporous part of Do & Do type equations
B	Distribution constant for Mahle equation
c	Henry's Law coefficient for DS equations
E_o	Reference energy
H	Proportionality constant in Talu–Meunier equation
K	Constant for Lagorsse equation
K_a	Langumuir-type constant for adsorption part of Lagorsse equation
K_{as}	Shape constant for CMMS equation
K_d	Langmuir-type constant for desorption part of Lagorsse equation
K_f	Langmuir-type constant for functional site part of Do & Do type equations
K_μ	Langmuir type constant for microporous part of Do & Do type equations
k	Constant for QHR equation
k_o	Langmuir-type constant for CMMS equations
k_1	Constant for CMMS equations
k_L	Langmuir constant
k_t	Constant in Talu–Meunier equation
N	Number of terms to sum
n	Dubinin–Astakhov exponent
n_I, n_V	Stoeckli exponents
p_{50}	Relative pressure at 50% of a_o adsorbed
p_r	Relative pressure of water (relative humidity)
R_g	Universal gas constant
T	Temperature

P.D. Sullivan (✉) · B.R. Stone
Airbase Technologies Division, Air Force Research Laboratory, 139 Barnes Dr Ste 2, Tyndall AFB, FL 32403, USA
e-mail: patrick.sullivan@tyndall.af.mil

Z. Hashisho · M.J. Rood
Department of Civil & Environmental Engineering, University of Illinois, Urbana, IL 61801, USA

Report Documentation Page

Form Approved
OMB No. 0704-0188

Public reporting burden for the collection of information is estimated to average 1 hour per response, including the time for reviewing instructions, searching existing data sources, gathering and maintaining the data needed, and completing and reviewing the collection of information. Send comments regarding this burden estimate or any other aspect of this collection of information, including suggestions for reducing this burden, to Washington Headquarters Services, Directorate for Information Operations and Reports, 1215 Jefferson Davis Highway, Suite 1204, Arlington VA 22202-4302. Respondents should be aware that notwithstanding any other provision of law, no person shall be subject to a penalty for failing to comply with a collection of information if it does not display a currently valid OMB control number.

1. REPORT DATE	2. REPORT TYPE	3. DATES COVERED
2007		**00-00-2007 to 00-00-2007**

4. TITLE AND SUBTITLE	5a. CONTRACT NUMBER
Water Adsorption With Hysteresis Effect Onto Microporous Activated Carbon Fabrics	5b. GRANT NUMBER
	5c. PROGRAM ELEMENT NUMBER
6. AUTHOR(S)	5d. PROJECT NUMBER
	5e. TASK NUMBER
	5f. WORK UNIT NUMBER
7. PERFORMING ORGANIZATION NAME(S) AND ADDRESS(ES) **Airbase Technologies Division,Air Force Research Laboratory,139 Barnes Dr Ste 2,Tyndall AFB,FL,32403**	8. PERFORMING ORGANIZATION REPORT NUMBER
9. SPONSORING/MONITORING AGENCY NAME(S) AND ADDRESS(ES)	10. SPONSOR/MONITOR'S ACRONYM(S)
	11. SPONSOR/MONITOR'S REPORT NUMBER(S)

12. DISTRIBUTION/AVAILABILITY STATEMENT
Approved for public release; distribution unlimited

13. SUPPLEMENTARY NOTES
U.S. Government or Federal Rights.

14. ABSTRACT

15. SUBJECT TERMS

16. SECURITY CLASSIFICATION OF:			17. LIMITATION OF ABSTRACT	18. NUMBER OF PAGES	19a. NAME OF RESPONSIBLE PERSON
a. REPORT	b. ABSTRACT	c. THIS PAGE			
unclassified	**unclassified**	**unclassified**	**Same as Report (SAR)**	**17**	

β Energy coefficient of an adsorbate–adsorbent system ($\beta E_o = E$, the affinity energy of the system)
β_I, β_V Energy coefficient of each term in the Stoeckli formula
κ Fitting parameter for Dubinin–Serpinsky type equations
ξ_i Fitting parameters for LeVan equation

1 Introduction

Understanding water vapor adsorption onto activated carbons is important for adsorption processes such as steam regeneration of activated carbons or the removal of contaminants from humid gas streams. Water can compete for available adsorption sites and reduce the capacity for the carbon to capture target compounds. Under high humidity, water can completely fill the micropores, nearly eliminating the capacity to capture any contaminants more weakly adsorbed than water (Huggahalli and Fair 1996). The coadsorption of water and organics onto GAC has been studied, including the hysteresis effect (Rudisill et al. 1992).

One relevant application for which contaminants are removed by adsorption from humid gas streams is providing protection against a chemical attack in either military or homeland defense (terrorist) situations. Whether purifying air with a respirator for personal protection, or purifying air with a filtration system for collective protection of a shelter or building, outside air is the medium to be filtered, and it is not humidity-controlled. Another application where outside air may be filtered is in large-scale painting operations, where exhaust volumes can range to the thousands of cubic meters per second, and the cost of humidity control is prohibitive.

Activated carbon fibers (ACFs) show great promise as a new adsorbent and catalyst support in competition with more-traditional activated carbons (Mays 1999). Carbon fibers can be woven into cloth and then activated to form activated-carbon-fiber cloth (ACFC). ACFCs are generally made from pitch, rayon, polyacrylonitrile (PAN), or phenolic (Novoloid, Hayes 1981) resin. The fibers are woven into a fabric and then activated in steam or CO_2 at high temperatures (e.g., 800 °C). ACFCs have the ability to be regenerated by direct electrical resistance heating. Resistance heating has been shown to be a more rapid and energy-efficient method of regenerating activated carbon than desorbing with steam or inert gas (Petkovska and Mitrovic 1994). Because of this, ACFCs have been studied recently in an effort to develop next-generation energy-efficient cyclic adsorption systems (Subrenat and Le Cloirec 2006; Vidal et al. 2006; Hashisho et al. 2007).

The reduced organic adsorption in humid gas streams onto ACFCs has been studied for both equilibrium (Cal et al. 1996) and dynamic (Sullivan et al. 2001) adsorption. Water adsorption isotherms are herein presented for a variety of ACFCs, and Calgon BPL as a reference, in an attempt to more thoroughly understand the adsorption of water onto these materials.

2 Experimental methodology

2.1 Carbon selection and sample preparation

Carbons examined in this study included Calgon BPL™ granular activated carbon (GAC), military ASZM–TEDA granular activated carbon (GAC) from a C2A1 respirator, Activated carbon nanofiber (ACnF), Calgon Zorflex™ activated carbon cloth, and Novoloid-based activated carbon fiber cloth (ACFC). The matrix of Novoloid-based ACFCs tested consisted of four levels of activation of virgin, oxidized, and H_2-treated fabrics.

The ACFC used was American Kynol ACC-5092-10, ACC-5092-15, ACC-5092-20, and ACC-5092-25. The last two digits of the ACFC part number are related to the level of activation and are analogous to the nominal surface area of the material, i.e., -10 is ~1000 m^2/g, -15 is ~1500 m^2/g, and so on. The Calgon Zorflex™ material tested was ACC-FM10 and ACC-FM10-700. The ACnF material used was produced by eSpin Technologies Inc., of Chattanooga, Tenn. The ACnF is a non-woven, produced by electrospinning polyacrylonitrile (PAN), and then activated by conventional means.

The oxidized samples were obtained by treating virgin ACFC samples (0.025 m^2, 4 to 7 g) having different grades of activation with 150 mL of 1/1 (V/V) concentrated HNO_3 and H_2SO_4 solution for 5 days (Dimotakis et al. 1995a, 1995b). Samples were then washed with distilled water until neutral pH conditions. Samples were then drained from water and dried in an oven at 150 °C in a flow of 200 sccm of N_2.

The H_2-treated ACFC samples were heated at 950 °C in pure hydrogen environment (Menendez et al. 1996; Li et al. 2002). Each sample was put in a quartz boat inside a 5-cm outer-diameter quartz tube fitted inside a temperature-controlled tube furnace (Lindberg furnace model 54232; temperature controller unit 59344). The samples were heated in N_2 for 2 hours at 200 °C to remove chemisorbed oxygen and then the gas was switched to hydrogen (Zero gas grade) at 200 sccm. The samples remained at 950 °C for 3 hours, then heating was stopped and the samples were left to cool down. When the temperature decreased below 100 °C, the blanketing gas was switched to N_2.

Samples were labeled according to the precursor followed by a suffix referring to the type of treatment, for instance -15V is untreated (virgin) ACC-5092-15, -15A is acid-treated (oxidized) ACC-5092-15, -15H is hydrogen-treated ACC-5092-15.

2.1.1 N_2 isotherms, surface area and pore size distribution

N_2 adsorption isotherms were generated by volumetric measurements using ASAP 2010 instrument (Micromeritics, Inc.). Samples were degassed for more than 8 hours at 150 °C under vacuum until a pressure of 4–6 μm Hg. Acid-treated samples have to be degassed for longer periods compared to the virgin or the hydrogen-treated samples to reach this degassing pressure limit. The adsorption isotherms were obtained at a relative pressure of 10^{-6} to 0.99. N_2 adsorption and desorption occurred at the N_2 boiling point (77 K).

The standard Brunauer–Emmett–Teller (BET) method was used to fit the adsorption data over a relative pressure range of 0.06 to 0.20. Micropore volume and pore size distribution were determined using the 3D model (Sun et al. 1998). The model is based on the Dubinin–Radushkevich (DR) equation and is used to model the adsorption of gases on microporous adsorbents with slit shaped pores between 4 Å and 100 Å. The average micropore width was determined based on pore size distribution for sizes ≤20 Å while the total pore volume was determined based on the volume of nitrogen adsorbed at saturation and using nitrogen liquid density (0.808 cm^3/g).

2.1.2 X-ray photoelectron spectroscopy (XPS)

The elemental content (C, O, N, and S) at the surface of the virgin and chemically treated ACFC samples was determined using XPS technique. The analysis was conducted using a PHI 5400 (Perkin–Elmer, Physical Electronics Inc.) instrument. A spot size of 1 mm^2 was targeted with Mg Kα radiation or Al Kα radiations at a power of 300 W at 15 kV under ultrahigh vacuum (10^{-8} to 10^{-9} torr).

2.1.3 H_2O adsorption isotherms

H_2O adsorption/desorption isotherms were collected gravimetrically with a Gravimetric Sorption Analyzer, Model GHP-F, manufactured by VTI Corporation of Hialeah, Fla. (Fig. 1). The system uses a Magnetic Suspension Balance by Rubotherm of Bochum, Germany. The matched mass flow controllers in the system are rated for a nominal 1.0 sLpm flow. Carbon samples used for the isotherms ranged from 40 mg to 150 mg.

Nitrogen was used as the carrier gas throughout the experiments. Each sample (except the ASZM–TEDA GAC) was dried at 250 °C under nitrogen prior to each isotherm until a static weight was achieved (<0.03% change in 10

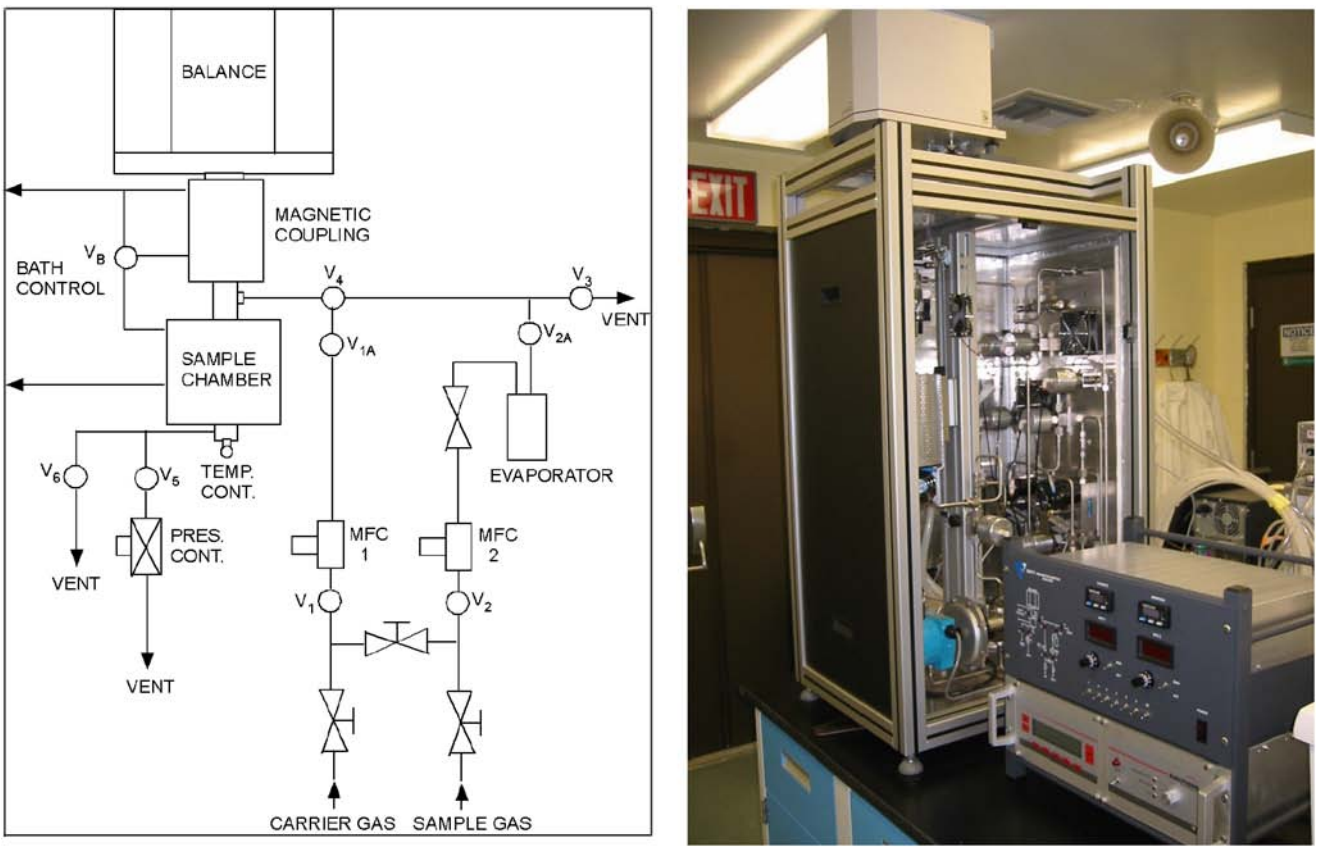

Fig. 1 Gravimetric sorption analyzer model GPH-F schematic and photo

minutes) or for a maximum time of one hour. The ASZM–TEDA carbon was dried at 105 °C to minimize impact on the impregnants in the carbon.

The GHP-F contains algorithms for generating a specified relative humidity (RH) based on the evaporator temperature, the sample temperature, the flow rates of the mass flow controllers, and a correlation for the vapor pressure of water. To verify the accuracy of the RH generated by the instrument, an Edgetech Vigilant™ Chilled-Mirror Hygrometer, with a model S3 sensor, was connected in series with the GHP-F. The set-point and measured RH values were within an average 1% RH. The total gas flow through the system was monitored with a mass flow meter, Omega FVL-1600 0–5 LPM.

3 Equilibrium isotherm modeling

A large collection of mathematical formulas have been proposed by previous investigators to model isotherms of adsorption. Here, we present an overview of equations that have been proposed to model adsorption of water onto carbon. Many of the more recently developed models have been fit to only a few sets of experimental data. While our approach to these formulas is genealogical, we will fit all these equations to our data to examine which equations better model the spectrum of materials.

We will attempt to elucidate the evolution from one formula to another and briefly state similarities of form to other equations. To make these similarities more clear, we have sometimes stated the equations in a different form from those given by the original authors. Quite a few recent equations take the form of a summation of two terms; these include the Stoeckli equation, all equations in the Do & Do family, and the extended CMMS equation. Oftentimes, when fit to a set of experimental data, one of the factors preceding the term representing how much of the adsorption that term is responsible for (represented by a with a subscript) will become zero or close to zero; this indicates that the term's contribution is insignificant, and overfitting is occurring. Usually if this factor is set to zero, the equation will reduce to a previously developed isotherm formula.

It is important to evaluate these models not only on a quantitative basis—that of measures of error and correlation—but also a qualitative basis. Mathematical qualities that should be satisfied including having a finite (usually nonzero) Henry's Law limit, some certain fixed values ($a = 0$ at $p_r = 0$, $a = a_o$ at $p_r = 1$), and increasing monotonically over the entire range of RH values. They should also be independent of units used. It is also worth mentioning that some formulas may fit to experimental data better more due to the flexibility of the form of their equation than to the theory used to derive them. If a formula is fit to a data set from a carbon with properties very different from the assumptions made in deriving the model, it may produce a good fit regardless, though the fitting parameters may not have physical meaning. This is increasingly common as the number of parameters to a formula becomes larger. Since many proposed formulas are modifications to previous formulas, we will group them and examine them as such.

In Table 1, p_r is the relative pressure of water (relative humidity), a is the amount adsorbed (in mg/g), T is temperature (in Kelvin), R_g is the universal gas constant, E_o is a reference energy, and N is a fixed value indicating how many terms to sum over. All other values, unless defined below, are treated as fitting parameters; except for ξ_i in the LeVan equation, all fitting parameters must be positive.

4 Dubinin–Radushkevich type formulas

The term 'micropore filling' was first coined in Dubinin's adsorption work; since micropore filling is important to these carbons, it is reasonable to start there. The original Dubinin–Radushkevich equation dates to 1947. The DR equation was found to perform well on most activated carbon, but not to deal well with carbons with very fine micropores (Do 1998, p. 156). The Dubinin–Astakhov equation replaces the exponent of 2 with n, a parameter that increases with the degree of activation.

The Stoeckli equation (Stoeckli 2002), created to fit type IV isotherms on oxidized carbon, is a sum of two DA equations, one to account for the type I behavior and one to account for the type V behavior.

The Doong–Yang equation (Doong and Yang 1987) is one of only two equations we have found that accounts for hysteresis in desorption. To model the desorption, h_o is set to the relative pressure at the beginning of the hysteresis loop. Gamma is an empirical activity coefficient, and is found using the Dubinin–Serpinsky equation DS2, which will be discussed in the next section.

All equations of this family have a Henry's Law limit of 0 (as long as $n > 1$) (Do 1998, p. 162), which many previous investigators have remarked is thermodynamically inconsistent. However, in very hydrophobic carbons, the value of the Henry's Law constant is very small, and this limit can be a reasonable approximation.

5 Dubinin–Serpinsky type formulas

The first four equations of DS type vary in the factor that is used to account for the decrease of available adsorption sites. DS2 was proposed by Dubinin (Dubinin and Serpinsky 1981), and DS4 by Barton et al. as a modification to the DS2 (Barton et al. 1992). There are members of the DS

Table 1

Dubinin–Radushkevich type formulas		
Dubinin–Radushkevich (DR)	$a = a_o \exp[-(\frac{A}{\beta E_o})^2],\ A = R_g T \ln \frac{1}{p_r}$	2nd order
Dubinin–Astakhov (DA)	$a = a_o \exp[-(\frac{A}{\beta E_o})^n]$	3rd order
Stoeckli	$a = a_I \exp[-(\frac{A}{\beta_I E_o})^{n_I}] + a_V \exp[-(\frac{A}{\beta_V E_o})^{n_V}]$	6th order
Doong–Yang (DY)	$a = a_o \exp(-(\frac{R_g T}{\beta E_o})^2[(\ln \frac{\gamma}{p_r})^2 - (\ln h_o)^2])$	4th order
Dubinin–Serpinsky type		
Dubinin–Serpinsky (DS2)	$p_r = \frac{a}{c(a_p+a)(1-\kappa a)}$	3rd order
DS4	$p_r = \frac{a}{ca_p+ca(1-\exp(-\kappa^2(a-a_c)^2))}$	4th order
LeVan	$p_r = \frac{a}{\sum_{i=0}^{N} \xi_i a^i}$	Nth order
Do & Do type		
Do & Do (DD)	$a = a_f \frac{K_f \sum_{i=1}^{N} i p_r^i}{1+K_f \sum_{i=1}^{N} p_r^i} + a_\mu \frac{K_\mu p_r^5}{1+K_\mu p_r^5}$	4th order
CIMF	$a = a_f \frac{K_f \sum_{i=1}^{m+1} i p_r^i}{1+K_f \sum_{i=1}^{m+1} p_r^i} + a_\mu \frac{K_\mu p_r^m}{1+K_\mu p_r^m}$	5th order
Cossarutto	$a = a_f \frac{K_f p_r}{1+K_f p_r} + a_\mu \frac{K_\mu p_r^m}{1+K_\mu p_r^m}$	5th order
Lagorsse	Adsorbing: $a = a_f \frac{1}{1+K_a p_r^7} \frac{\sum_{i=1}^{7} i(K p_r^i)}{1+\sum_{i=1}^{7}(K p_r^i)} + a_\mu \frac{K_a p_r^7}{1+K_a p_r^7}$	5th order
	Desorbing: $a = a_f \frac{1}{1+K_d p_r^7} \frac{\sum_{i=1}^{7} i(K p_r^i)}{1+\sum_{i=1}^{7} i(K p_r^i)} + a_\mu \frac{K_d p_r^7}{1+K_d p_r^7}$	
Other		
Qi–Hay–Rood (QHR)	$a = \frac{a_o}{1+\exp[k(p_{50}-p_r)]}$	3rd order
Mahle	$a = a_o \frac{\arctan(\frac{p_r - A}{B}) - \arctan(\frac{-A}{B})}{\arctan(\frac{1-A}{B}) - \arctan(\frac{-A}{B})}$	3rd order
Talu–Meunier	$p_r = \frac{H\Psi}{1+k\Psi} \exp(\Psi/a_m),\ \Psi = \frac{-1+\sqrt{1+4k\zeta}}{2k},\ \zeta = \frac{a_m a}{a_m - a}$	3rd order
CMMS	$a = a_o \frac{k_o p_r}{(1-K_{as})(k_o p_r + w^2(1-K_{as}))},$	
	$w = \frac{1}{2}(1 - \frac{k_1 p_r}{(1-K_{as})} + \sqrt{(1 - \frac{k_1 p_r}{(1-K_{as})})^2 + \frac{4k_o p_r}{(1-K_{as})}})$	4th order
CMMS Type V (Ising)	$a = a_o \frac{k_o p_r}{k_o p_r + w^2},\ w = \frac{1}{2}(1 - k_1 p_r + \sqrt{(1-k_1 p_r)^2 + 4k_o p_r})$	3rd order
Extended CMMS (Ising–Langmuir)	$a = a_L \frac{k_L p_r}{1+k_L p_r} + a_I \frac{k_o p_r}{k_o p_r + w^2}$, w as used in the Ising equation	5th order

family we have chosen not to treat. DS1 (Dubinin 1980) fits poorly to data at middle-to-high RH and is not treated here. DS3 (Barton et al. 1991) claims that the relative humidity when $a = 0$ is usually more than 1/3, and that the derivative $\mathrm{d}a/\mathrm{d}p$ there is large; this is clearly aphysical. The Corrected DS equation (CDS) (Gauden 2005) was proposed by Gauden and contains an extended empirical factor to improve on DS4 at relative pressures less than 10%, but due to the limitations of our experimental system, we do not have adsorption data at relative pressures between 0% and 10%. The CDS can also be shown to not be independent of units, because of logarithms and exponentials in its formula. For these reasons we have chosen not to treat these equations.

The LeVan equation (Qi and LeVan 2005) is a very flexible formula that is essentially a truncated power series of n/p in terms of n. It is included here because the derivation follows that of the DS equations, and it contains the DS2 and DS3 equations as special cases ($N = 2$ and $N = 3$, respectively). It is also evident that if N was allowed to tend to infinity, it would be able to contain the DS4 and the CDS equations, as well as, in theory, any other isotherm formula. Usually $N = 4$ is enough to get a good fit. Aside from ξ_o, which is the Henry's Law constant, the physical meaning of other parameters to the equation is not clear. Also, because of its flexibility, care must be taken to make sure that its parameters are such that the equation is increasing and positive throughout its domain.

The stated form of these equations, which give the relative humidity in terms of the loading, is the opposite of the usually desired form and is awkward to use in practice. DS2 can be stated to give the loading in terms of the RH by solving a quadratic, but this form is somewhat unwieldy; since

for purposes of fitting the two equations are equally useful, we have chosen to use the stated form.

6 Do & Do type formulas

The equation of Do and Do (2000) to model water isotherms has received a good deal of attention since its proposal. One of Do & Do's key assumptions is that water inside micropores forms clusters of molecules. The original Do & Do (DD) formula assumes clusters of 5. The CIMF isotherm, proposed shortly afterwards, generalized Do's equation to clusters of arbitrary size, and Cossarutto's modification to the DD formula went one step further and simplified the portion of the equation representing adsorption on functional groups. The first term in these three models is a SIPS equation, and the second term of Cossarutto's equation is a Langmuir isotherm.

Lagorsse et al. proposed the second formula that accounts for desorption (Lagorsse et al. 2005). They follow a similar derivation to the DD equation, but assume clusters of 7 molecules. The first term of both equations of the Lagorsse formula is also a SIPS isotherm.

Furmaniak et al. proposed a "Heterogeneous Do–Do Model" that accounts for different energies of adsorption at different functional sites (Furmaniak et al. 2005). However, without prior knowledge of the nature of functional sites on the material, one must make guesses as to the number and properties of the sites the material may have. Since we, unfortunately, do not have that knowledge, we have chosen to not treat this model in our paper.

We note that the summands in these equations have explicit forms that simplify computation.

7 Other formulas

The Qi–Hay–Rood formula is another type 5 model, derived to be an improvement on the DS4 equation. The QHR is nonzero at $p_r = 0$, but its value there is very close to zero (Qi et al. 1998).

Mahle proposes a type 5 formula, based on the assumption that the pore distribution approximates a Cauchy distribution, which is similar in shape to a normal distribution (Mahle 2002). It is known that the pore distribution in activated carbons is often bimodal, so this assumption may not always hold. The general method for deriving an isotherm from a distribution of pore sizes is discussed in chapter 3.10 of *Adsorption Analysis: Equilibria and Kinetics* (Do 1998).

Talu and Meunier derived a type V isotherm that assumes water molecules are more attracted to each other than to the carbon, and therefore once water is adsorbed to a functional group other waters will cluster onto that original water molecule (Talu 1996).

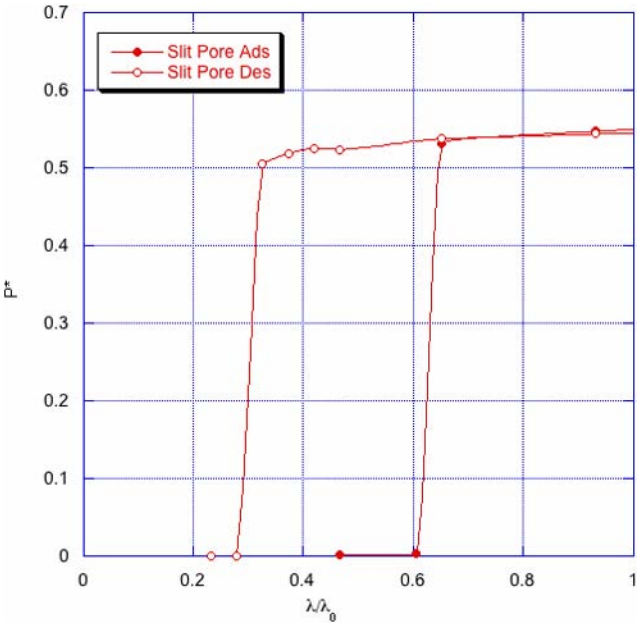

Fig. 2 Water vapor isotherms with the SPC model for slit pores of 0.65 nm (Liu and Monson 2006). Reproduced with permission

Rutherford proposed a model based on cooperative multimolecular sorption theory (CMMS) that explains well the effects of interaction with functional sites, but does not account for microporosity or condensation, and does not work well at relative humidities above 80% (Rutherford 2003). The CMMS model can account for type II and type V isotherms. Assuming a type V isotherm, the CMMS model reduces to an equation called the Ising equation. Rutherford also proposed an Extended CMMS model to better examine carbons with minimal micro- or nanoporosity (Rutherford 2006). The form of the extended CMMS equation is a sum of an Ising equation and a Langmuir equation.

8 Molecular simulations of adsorption

With increasing amounts of computational power available to the researcher, molecular simulations of adsorption have become more popular. Earlier work is summarized by Brennan (Brennan et al. 2001). More recently, Liu & Monson using the Gibbs Ensemble Monte Carlo (GEMC) method produced isotherms for a carbon assumed to consist of slit pores with no active sites, and postulated that a microporous, hydrophobic carbon would resemble their isotherms (Liu and Monson 2005). We will later show that the isotherms for our hydrogen-treated Kynol™ material bear certain similarities to these idealized molecular simulations.

In a more recent paper, Liu and Monson performed Monte Carlo simulations on a carbon made up of graphite platelets with randomly distributed active sites. The isotherms from those simulations strongly resemble the iso-

therms of Calgon BPL and similar carbons (Liu and Monson 2006).

9 Results and discussion

9.1 XPS of virgin and chemically treated ACFC

Oxidizing the ACF enriches the ACFC with oxygen-containing functional groups such as carboxylic acids, quinones, and phenolic hydroxides. Treating the ACFC samples with the mixture of concentrated HNO_3 and H_2SO_4 increased the average oxygen content among the samples from 4.5% to 23.9% while the average carbon content decreased from 94.7% to 74.6%. The average nitrogen content increased from 0.5% to 1.2% while the average sulfur content increased from 0.21 to 0.25%. Since the change in the sulfur and nitrogen content of the oxidized samples was small and disproportionate to the increase in the oxygen content, this indicates that the increase in oxygen content is not due to sulfate or nitrate groups from H_2SO_4 or HNO_3. On the other hand, heating the ACFC samples at 950 °C in UHP H_2 decreased the average oxygen content among the samples from 4.5% to 1.5%, the average nitrogen content from 0.5% to 0.4% while the average carbon content increased from 94.7% to 98.1%. For acid and hydrogen treatments, the change in oxygen content didn't seem to depend on the activation level of the virgin ACFC samples.

9.2 N_2 adsorption, surface area, and pore size distribution of virgin and chemically treated ACFC

The H-treated ACFC depicted comparable BET surface area to virgin ACFC. Going from ACFC10 to ACFC25, the BET surface area increased for both the virgin and the H-treated ACFC. On the other hand, BET area was comparable for all the oxidized ACFC, and was lower than that of virgin ACFC. The BET area for the oxidized ACFC was not related to the level of activation of the precursor virgin ACFC.

As is the case for BET surface area, the micropore and total pore volumes for the hydrogen treated samples were comparable but slightly lower than that for the virgin samples, while the acid treated samples depicted much lower micropore and total pore volumes compared to the virgin samples. In terms of ratio of micropore to total pore volume, the acid-treated samples depicted a reduction in microporosity for all ACFC activation levels. The hydrogen-treated samples manifested reduction in microporosity, particularly for ACFC10H and ACFC25H.

For all ACFC grades, acid treatment resulted in more change in mesopore size distribution compared to hydrogen treatment. Acid treatment increased the mesopore size. Such change resulted in increasing the average pore size

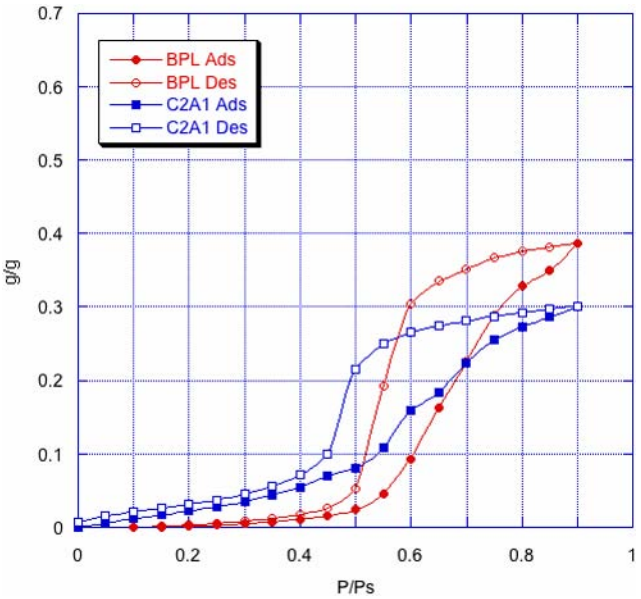

Fig. 3 Water vapor isotherms at 25 °C on Calgon BPL and ASZM–TEDA (C2A1)

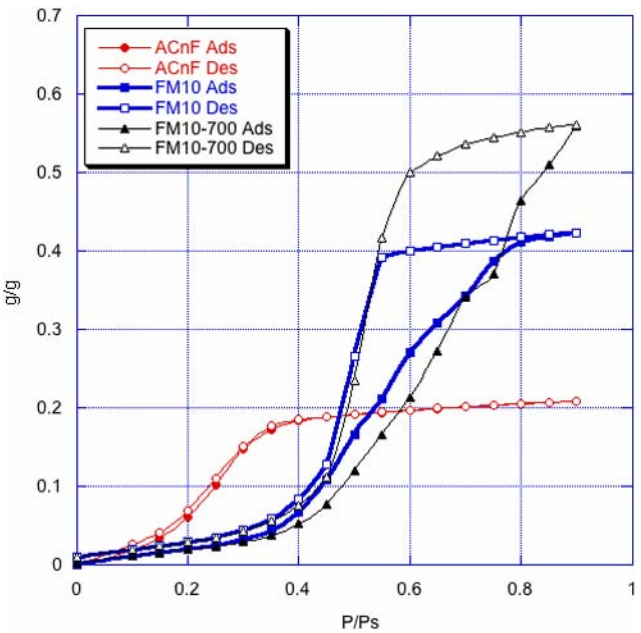

Fig. 4 Water vapor isotherms at 25 °C on ACnF, FM10, and FM10-700

of the acid-treated ACFC. On the other hand, hydrogen treatment doesn't seem to affect the mesopore size distribution. With respect to the micropore size distribution, the impact of acid treatment was most pronounced for ACFC20 and ACFC25 while ACFC10 and ACFC15 depicted smaller change in both micropore and mesopore size distributions. For all ACFC grades, micropore volume was much larger than the mesopore volume reflecting the high microporosity of ACFC.

Table 2 ACFC composition as determined by XPS

Sample name	Carbon (%)	Oxygen (%)	Nitrogen (%)	Sulfur (%)
ACFC-10V	94.1	5.4	0.3	0.3
ACFC-15V	95.3	3.6	1.0	0.1
ACFC-20V	94.2	4.8	0.6	0.3
ACFC-25V	95.4	4.3	0.2	0.2
ACFC-10A	75.1	23.8	0.9	0.2
ACFC-15A	74.4	24.3	1.0	0.2
ACFC-20A	72.6	25.3	1.8	0.3
ACFC-25A	76.4	22.3	1.2	Not available
ACFC-10H	98.4	1.2	0.4	Not available
ACFC-15H	98.7	1.1	0.2	Not available
ACFC-20H	97.8	1.6	0.6	Not available
ACFC-25H	97.5	2.1	0.4	Not available

Table 3 Characterization of ACFC samples using N_2 adsorption

Sample	BET surface (m^2/g)	Micropore volume (cm^3/g)	Total pore volume (cm^3/g)	Microporosity (%)	Average micropore size (nm)	Average pore size (nm)
ACFC10-V	849	0.40	0.40	99.3	0.67	0.67
ACFC15-V	1335	0.62	0.64	96.6	0.76	0.76
ACFC20-V	1566	0.74	0.76	97.5	0.84	0.86
ACFC25-V	1763	0.83	0.84	98.9	0.88	0.88
ACFC10-O	793	0.33	0.38	86.1	0.70	0.73
ACFC15-O	994	0.45	0.49	91.9	0.82	0.94
ACFC20-O	668	0.29	0.33	85.2	0.82	1.08
ACFC25-O	873	0.37	0.44	85.0	0.85	1.11
ACFC10-H	926	0.39	0.44	88.4	0.71	0.71
ACFC15-H	1314	0.60	0.62	95.6	0.80	0.80
ACFC20-H	1509	0.70	0.72	97.6	0.86	0.86
ACFC25-H	1739	0.77	0.83	93.1	0.88	0.88

While the average micropore size was less influenced by the chemical treatment, the average pore size for pores between 4 and 100 Å was much larger for acid-treated. This confirms the above suggestion that acid treatment resulted in micropores fusing together to form larger pores. On the other hand, both virgin and hydrogen-treated samples depicted similar average micropore and total pore sizes indicating small influence of hydrogen and heat treatment on the pore structure of ACFC. The decrease in the micropore volume and the absence of prominent effect on the micropore size is consistent with previous results reported by other researchers (Mangun et al. 1999).

To summarize, hydrogen treatment has very small impact on micropore and total pore volumes, average micropore size, BET surface area. On the other hand, acid treatment decreases the micropore and total pore volumes, microporosity, BET surface area. However acid treatment increases the average pore size and doesn't have significant effect on the micropore size. Hence, these results suggest that the addition of oxygenated functional groups by treatment with HNO_3 and H_2SO_4 mixture resulted in decreasing the volume accessible to N_2. It might be that the functional groups have blocked the pores of the ACFC. The large micropores which are readily accessible to nitrates and sulfate ions might be affected more by pore blockage than the small micropores that might be less accessible to those ions. This can justify the reduction in the micropore and total pore volumes. The increase in the mesopore size might be explained by the action of the concentrated acid in etching the carbon structure and/or by fusion of large micropores and small mesopore forming larger pores.

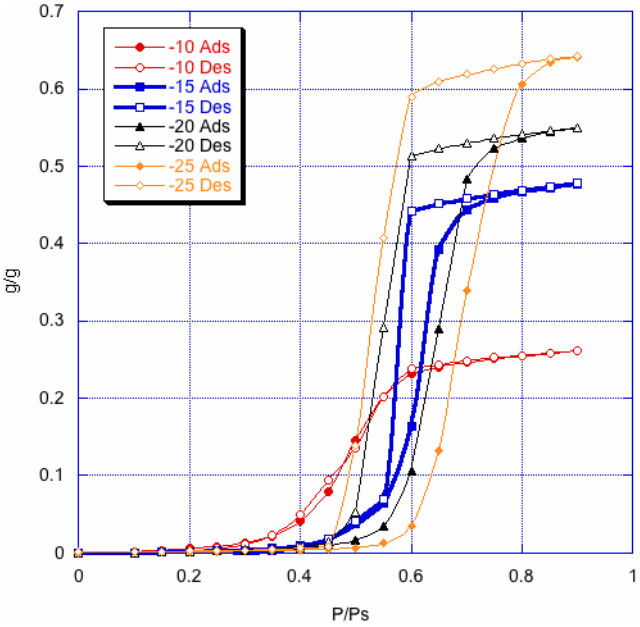

Fig. 5 Water vapor isotherms at 25 °C on ACC-5092-10, -15, -20, and -25

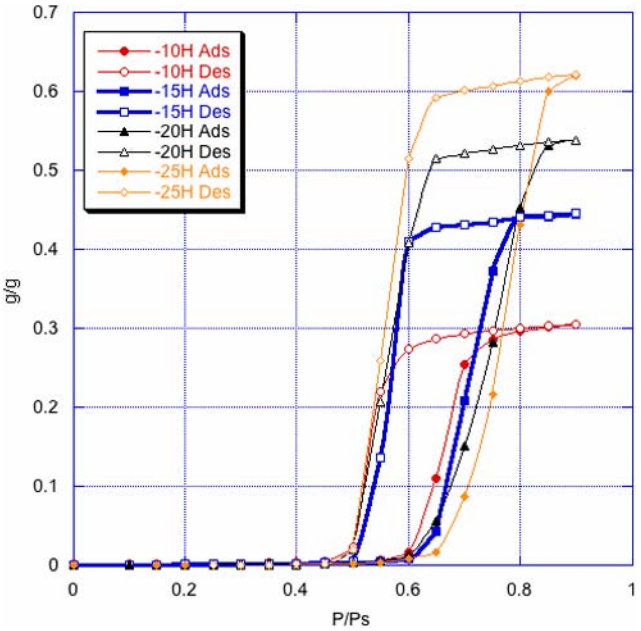

Fig. 7 Water vapor isotherms at 25 °C on hydrogen-treated ACC-5092-10, -15, -20, and -25

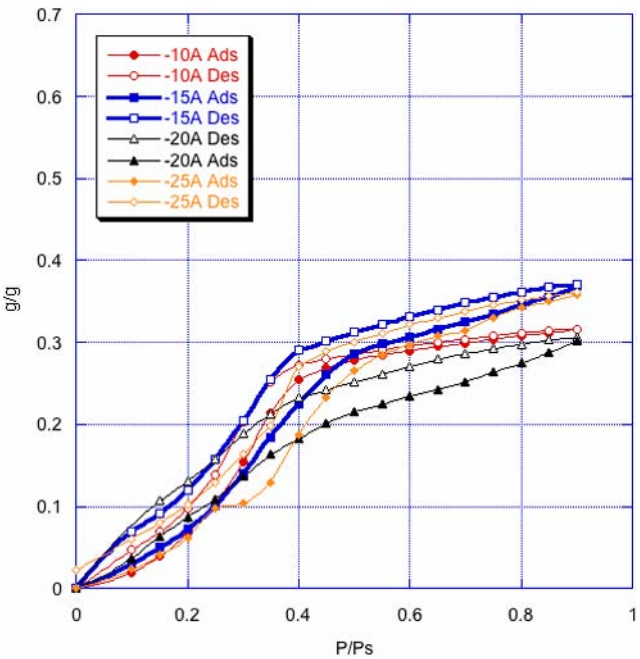

Fig. 6 Water vapor isotherms at 25 °C on acid-treated ACC-5092-10, -15, -20, and -25

9.3 Water adsorption isotherm results

Isotherm plots for the various carbons are presented in Figs. 3–7.

The BPL isotherm is in good agreement with previously published results (Huggahalli and Fair 1996; Rudisill et al. 1992). The ASZM–TEDA carbon is BPL with impregnants added to enhance adsorption of chemical warfare agents. The impregnants add primary adsorption sites and reduce the total pore volume. Thus the onset of water adsorption for the ASZM–TEDA is earlier, and the total water adsorption is reduced compared to the BPL.

The ACnF exhibits minimal hysteresis and is the most hydrophilic of all the carbons tested. Because the precursor of this material is PAN, the material likely has more primary adsorption sites than the non-nitrogen containing carbons. Preliminary XPS results for ACnF show 8% total nitrogen.

The Calgon Zorflex™ FM10 and FM10-700 use rayon as a precursor. Their curves most closely resemble those of BPL, whose starting material also contains a significant quantity of cellulose structures.

The Kynol™ ACFCs exhibit a strong type 5 isotherm according to IUPAC classification. This is characterized by low adsorption capacity at low RH followed by a sharp rise and then a plateau with little increase in adsorption capacity with increasing relative humidity. The degree of hysteresis increases with the level of activation. The shape of the ACFC isotherms most closely resemble those of pitch-based carbons examined by Kaneko et al. (Kimura et al. 2004; Ohba and Kaneko 2007). This is expected, as the pitch and phenolic resin carbons are chemically similar, as in the case of the BPL and Zorflex™. The Kynol™ is a slightly more homogenous material, and so the highly activated samples exhibit more idealized behavior, specifically the separation at the bottom of the hysteresis loop is greater.

The oxidation of the ACFCs transformed the isotherms from type 5 IUPAC classification to type 4. The materials were drastically modified in both chemical composition and

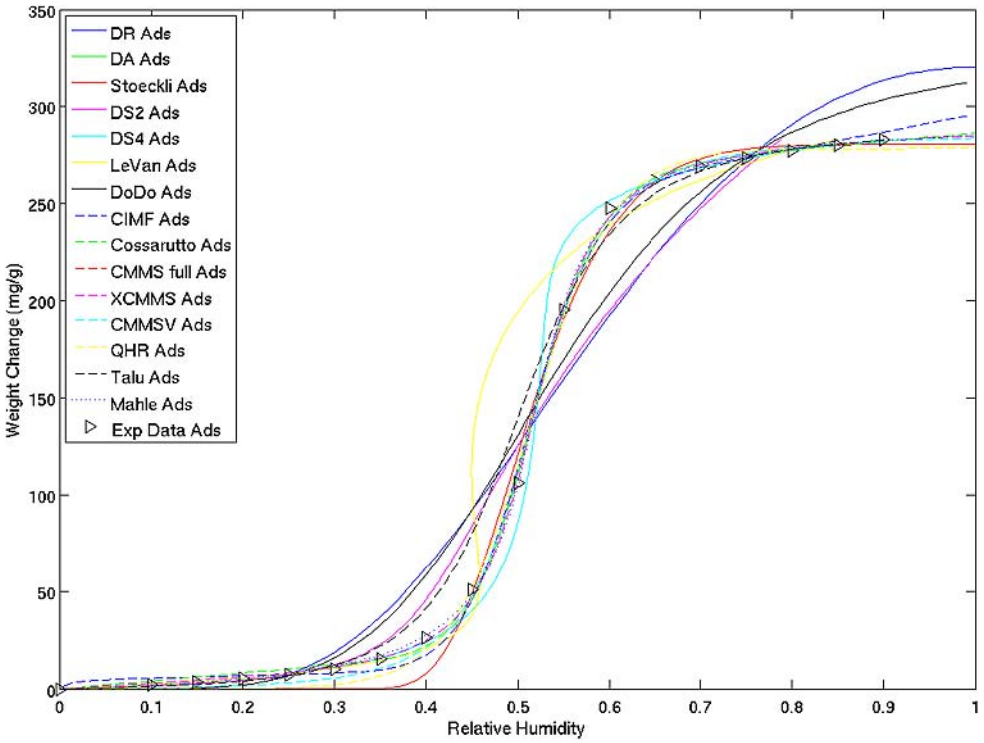

Fig. 8 Water vapor adsorption isotherms at 25 °C on virgin ACC-5092-10, with plots of fitted equations

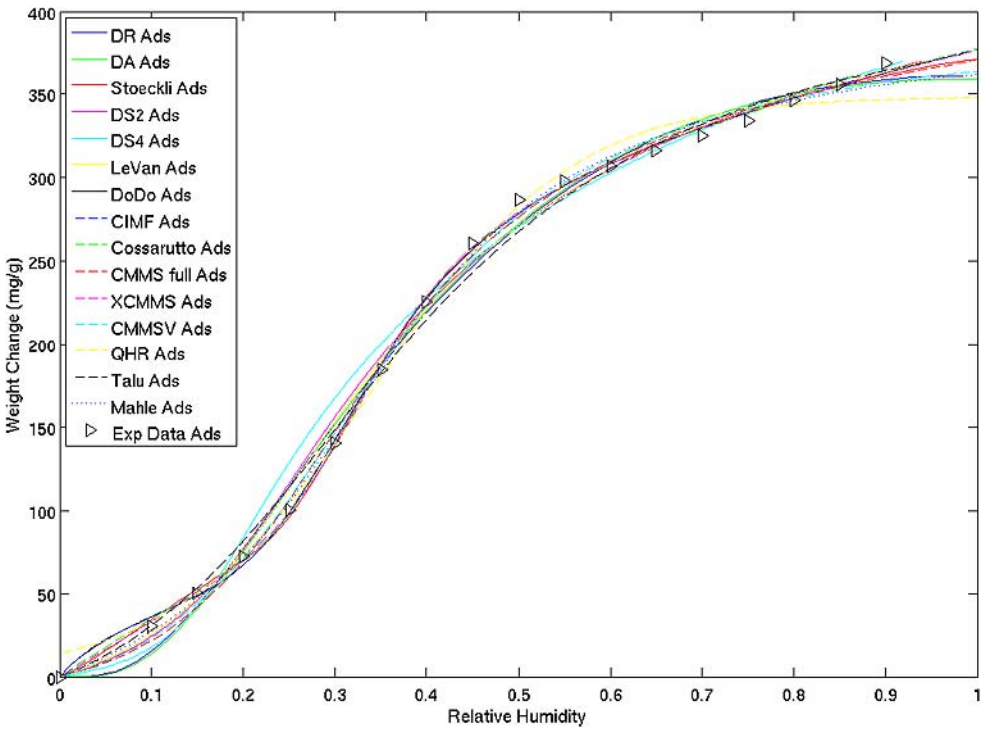

Fig. 9 Water vapor adsorption isotherms at 25 °C on acid-treated ACC-5092-15, with plots of fitted equations

pore structure as noted in Table 3, and the isotherms reflect this. With >20% oxygen, the primary adsorption sites are plentiful and water adsorption increases with increasing RH throughout the isotherm. Although this treatment yields increased water adsorption in high-humidity situations, which may be undesirable, it has utility in also increasing adsorption of other difficult-to-adsorb compounds, such as hydrides (Mangun et al. 1999).

The hydrogen-treated ACFCs have increased hydrophobicity. The -10 material is most radically changed, going from negligible hysteresis to significant hysteresis. As the pore size is relatively unchanged, this is an indication that

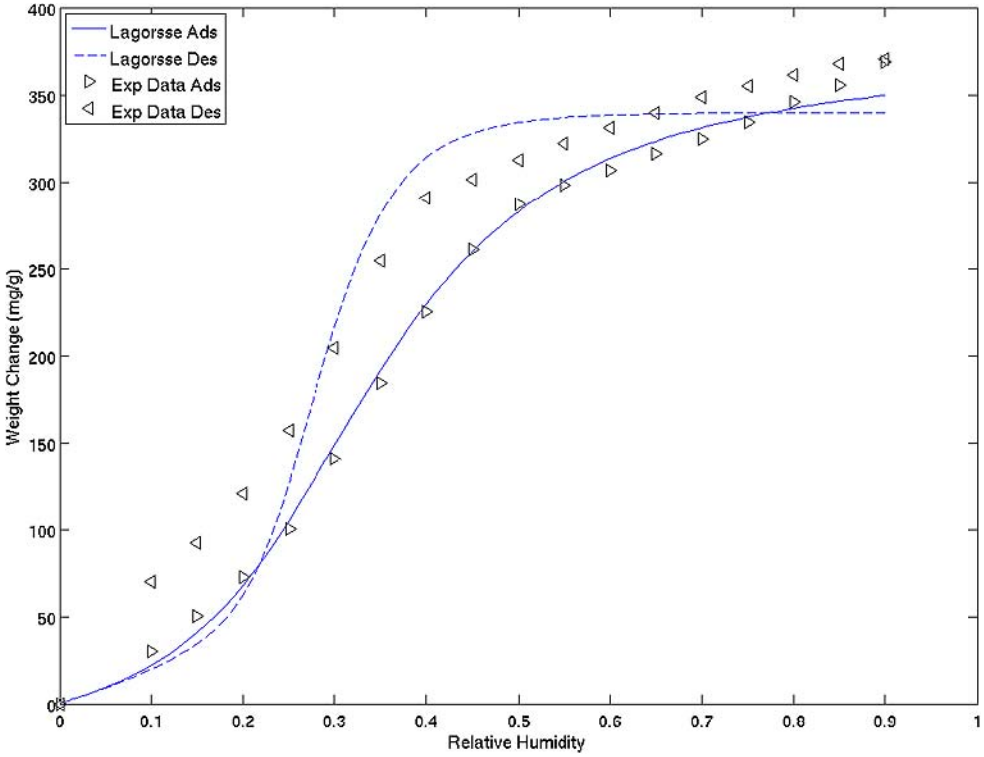

Fig. 10 Water vapor adsorption and desorption isotherm at 25 °C on acid-treated ACC-5092-15, with plots of fitted equations

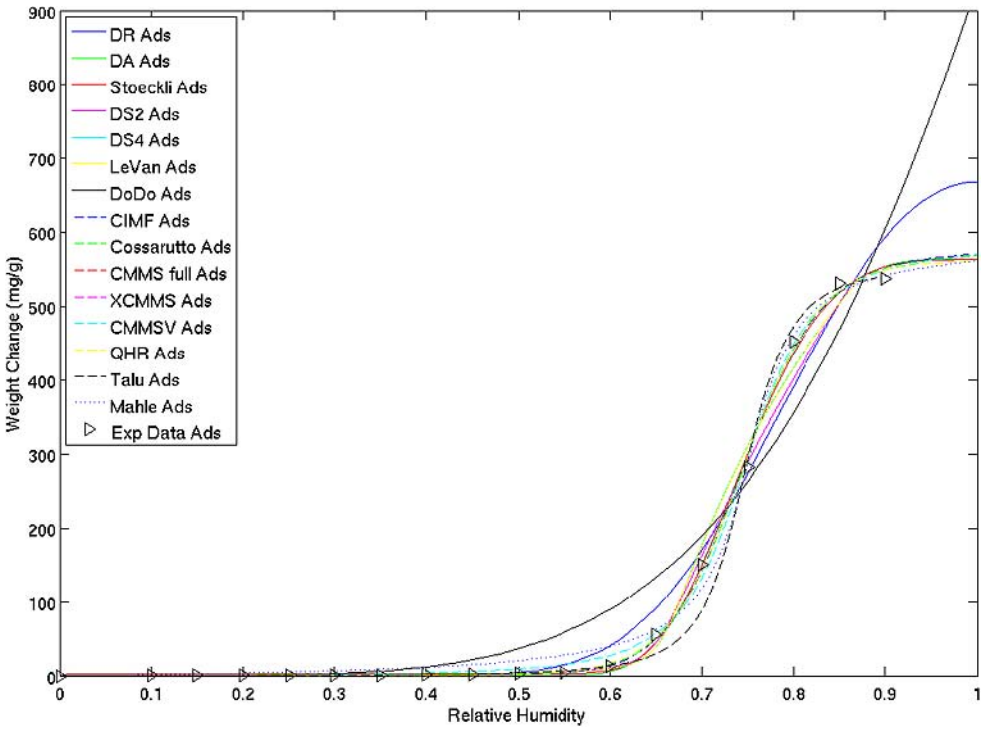

Fig. 11 Water vapor adsorption isotherms at 25 °C on hydrogen-treated ACC-5092-20, with plots of fitted equations

the surface chemistry is key to the transformation. The -15 material also is altered significantly, with the hysteresis loop being widened at the base. The -20 and -25 materials show a less dramatic general widening of the hysteresis loop.

When Figs. 2 and 7 are compared, it is apparent that the hydrogen-treated Kynol™ ACFC is more similar to the idealized slit-shaped pore model than previously studied carbons. The hysteresis loop is wider and more squared at the bottom of the loop. The plateau is of a similar shape and

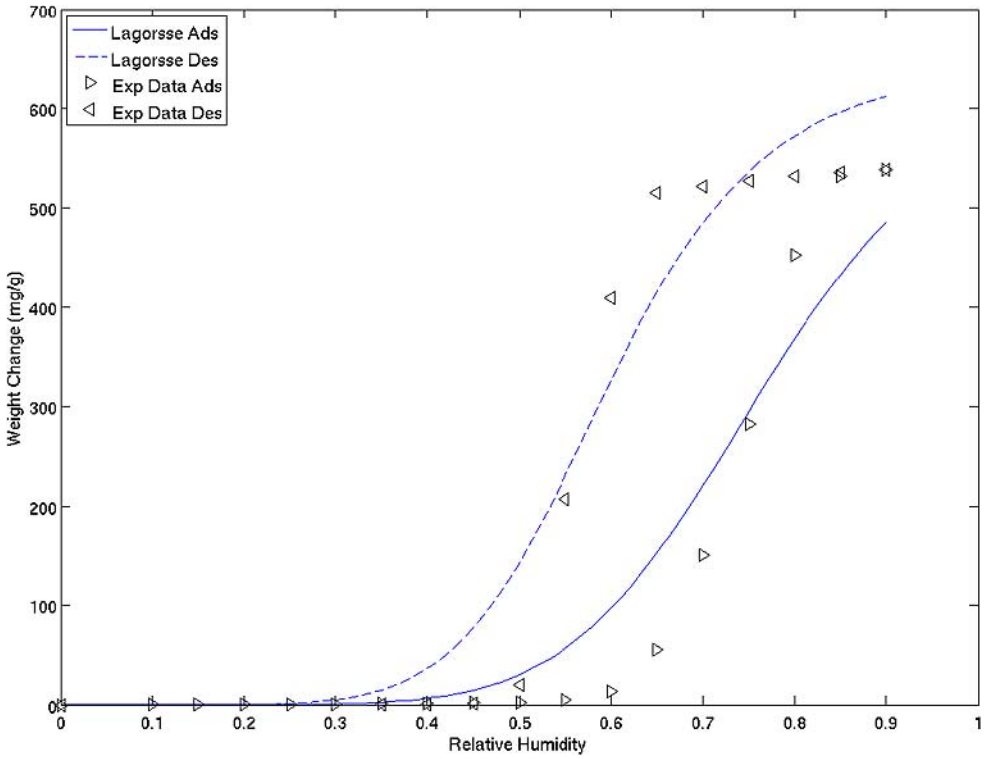

Fig. 12 Water vapor adsorption and desorption isotherms at 25 °C on hydrogen-treated ACC-5092-20, with plots of fitted equations

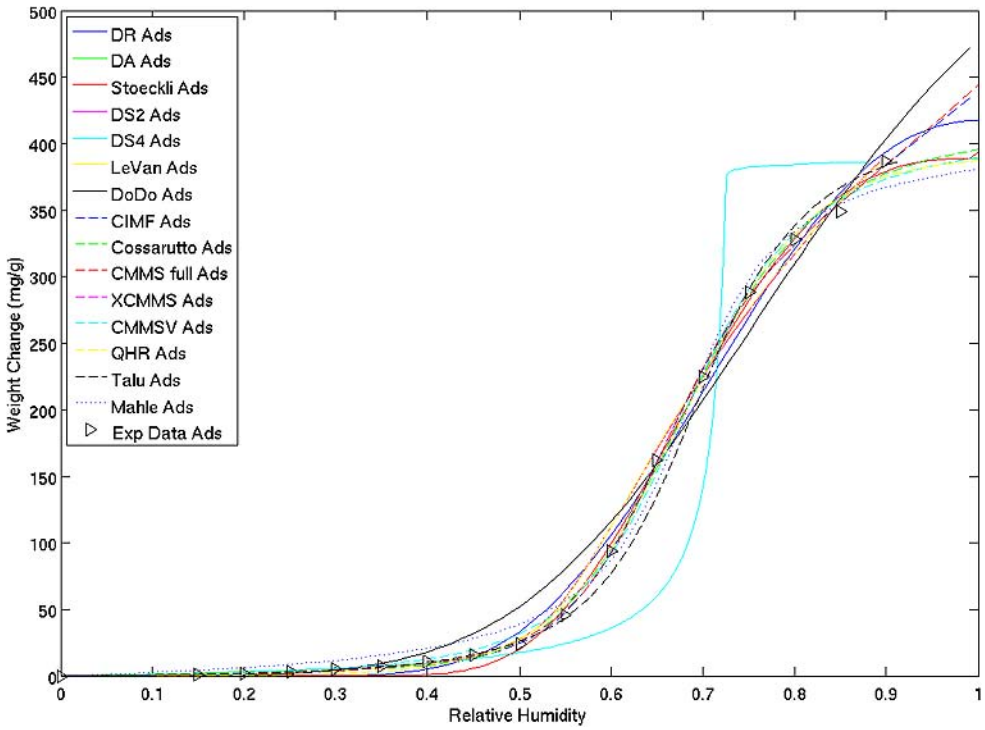

Fig. 13 Water vapor adsorption isotherm at 25 °C on Calgon BPL, with plots of fitted equations

slope. The adsorption loops commence adsorption around an RH of 60%.

The Liu and Monson model predicts that if there are no primary adsorption sites, condensation can still occur in the pore below the saturation pressure if the pore width is optimal—about 0.65 nm. The ACFCs have a pore size distribution that is not homogenous, and so there are some pores at this optimal size. The water that con-

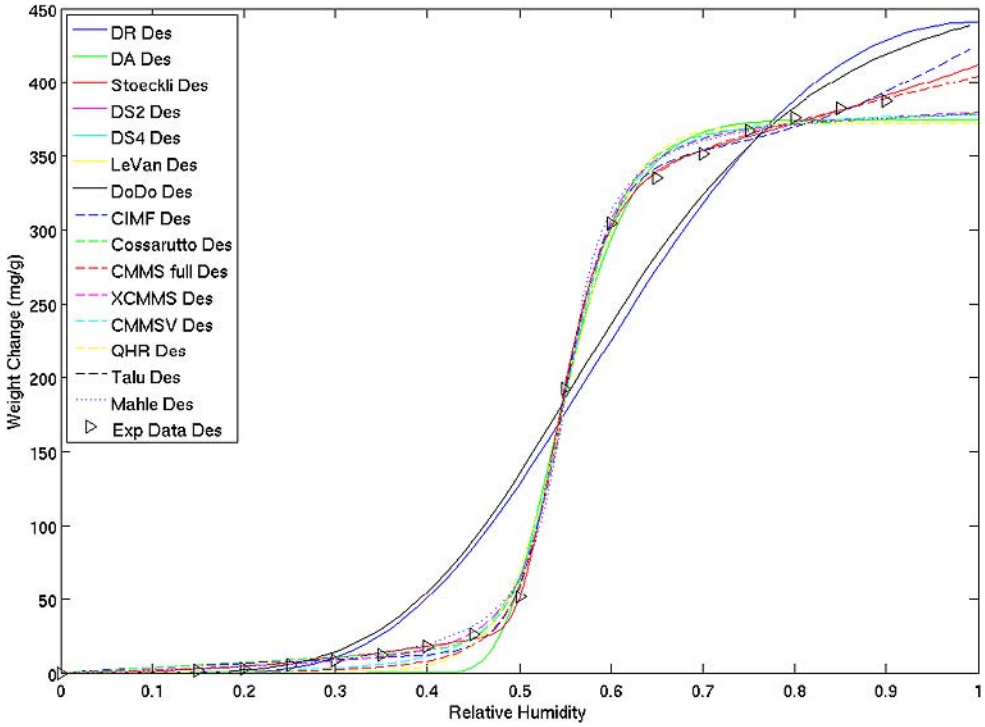

Fig. 14 Water vapor desorption isotherm at 25 °C on Calgon BPL, with plots of fitted equations

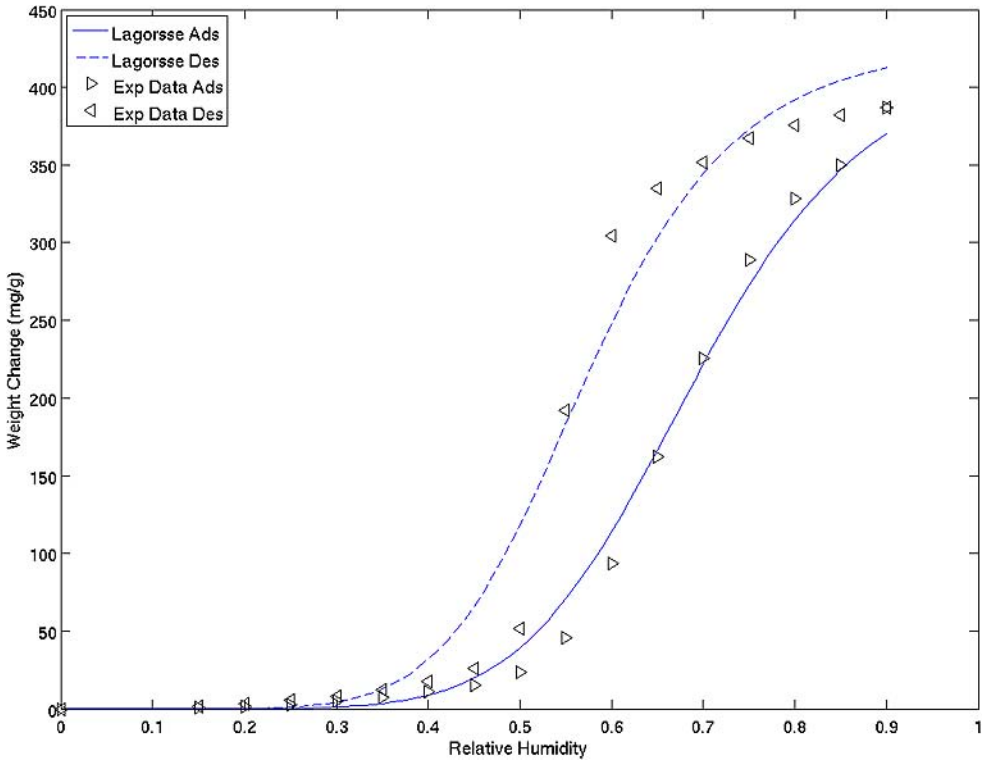

Fig. 15 Water vapor adsorption and desorption isotherm at 25 °C on Calgon BPL, with plots of fitted equations

denses in the optimal pores then becomes a secondary adsorption site for further water adsorption. Thus, significant water adsorption would generally commence at a RH of ∼60% in all supermicroporous materials regardless of the surface chemistry, based on the GEMC model.

10 Equilibrium isotherm modeling results

We applied a least squares fitting algorithm to the equations listed in Table 1, and calculated the r^2 values of the equations against the experimental data. The results are summarized in Table 4.

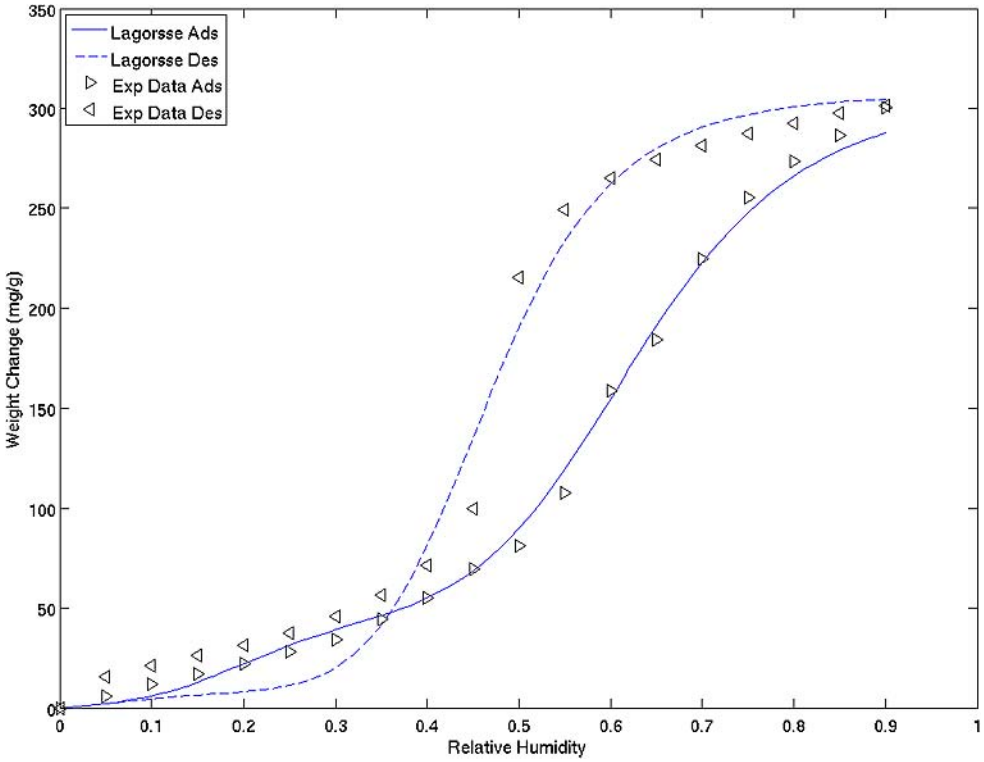

Fig. 16 Water vapor adsorption and desorption isotherm at 25 °C on ASZM–TEDA, with plots of fitted equations

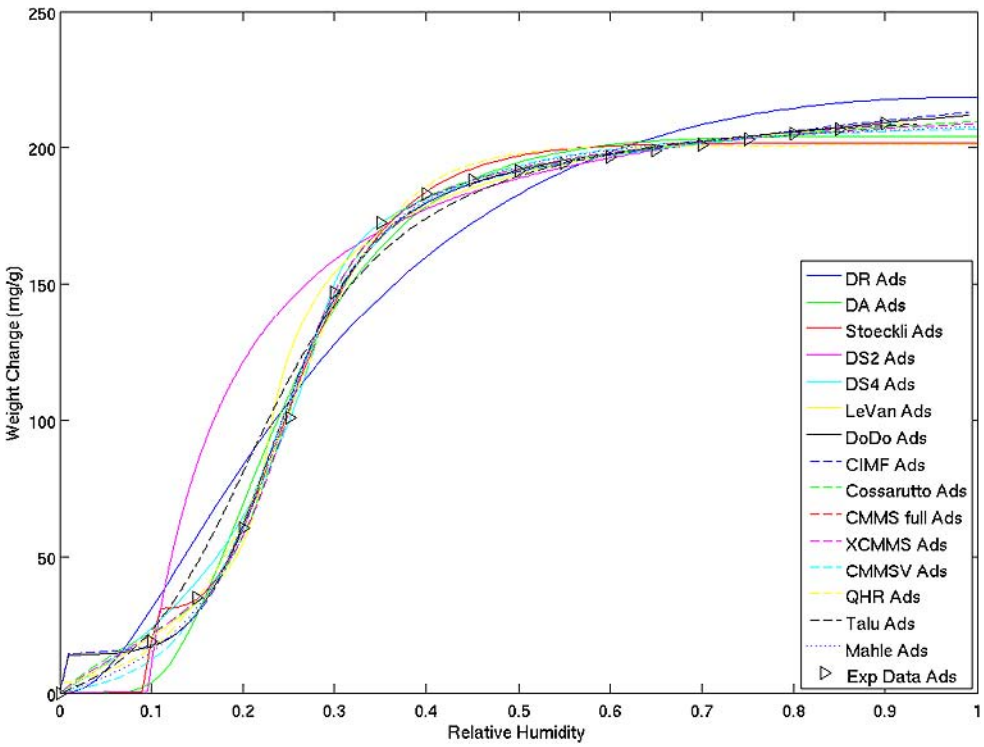

Fig. 17 Water vapor adsorption isotherm at 25 °C on eSpin ACnF, with plots of fitted equations

Most equations seem to fit well, at least numerically, to the hydrophilic carbons. It can be seen from Table 4 that the virgin and hydrogen-treated Kynol™ fabrics have overall worse correlation with these equations than the other adsorbent materials. There are, however, some equations that do well on both: the CMMS-type equations and the Stoeckli, CIMF, QHR, Talu–Meunier, and Mahle equations all have minimum r^2 values of greater than 99% for this data set. In fact, the largest r^2, 99.99%, occurs for one of these hydrophobic carbons with the full CMMS equation.

Table 4 The regression coefficient r^2 for each pair of equation and experimental data

	DR	DA	Stoeckli	DS2	DS4	LeVan	DoDo	CIMF	Cossarutto
ACnF	95.53%	99.18%	99.61%	98.23%	99.85%	99.39%	99.81%	99.81%	99.93%
ASZM–TEDA Canister	98.76%	98.79%	99.86%	99.14%	99.75%	99.93%	99.57%	99.79%	99.86%
BPL	99.49%	99.83%	99.78%	99.36%	93.59%	99.31%	98.25%	99.95%	99.88%
Zorflex FM10	99.65%	99.70%	99.90%	98.86%	99.37%	99.42%	99.83%	99.88%	99.88%
Zorflex FM10-700	99.14%	99.70%	99.62%	99.32%	99.31%	99.31%	99.78%	99.79%	99.79%
ACFC10V	95.05%	99.62%	99.51%	95.40%	99.86%	98.47%	96.21%	99.84%	99.94%
ACFC15V	94.75%	99.60%	99.49%	97.91%	99.46%	98.41%	92.69%	99.79%	99.90%
ACFC20V	94.54%	99.77%	99.71%	98.28%	99.58%	98.81%	91.56%	99.90%	99.93%
ACFC25V	93.13%	99.95%	99.94%	97.78%	89.25%	98.42%	88.79%	99.93%	99.93%
ACFC10H	92.82%	99.89%	99.97%	97.47%	98.79%	98.02%	88.37%	99.94%	99.94%
ACFC15H	94.26%	99.94%	99.93%	98.68%	93.37%	98.77%	88.39%	99.95%	99.96%
ACFC20H	98.26%	99.77%	99.70%	99.54%	99.52%	99.52%	93.49%	99.81%	99.82%
ACFC25H	98.15%	99.73%	99.69%	98.10%	89.93%	98.13%	92.09%	99.80%	99.81%
ACFC15A	99.36%	99.33%	99.84%	99.27%	98.98%	99.22%	99.87%	99.85%	99.89%
Max	99.65%	99.95%	99.97%	99.54%	99.86%	99.93%	99.87%	99.95%	99.96%
Min	92.82%	98.79%	99.49%	95.40%	89.25%	98.02%	88.37%	99.79%	99.79%

	Lagorsse	CMMS full	XCMMS	CMMSV	QHR	Talu	Mahle	Max	Min
ACnF	99.12%	99.73%	99.85%	99.75%	99.58%	98.61%	99.87%	99.93%	95.53%
ASZM–TEDA Canister	98.71%	99.45%	99.87%	99.49%	99.46%	98.92%	99.76%	99.93%	98.71%
BPL	98.01%	99.94%	99.78%	99.82%	99.84%	99.50%	99.50%	99.95%	93.59%
Zorflex FM10	98.68%	99.83%	99.83%	99.84%	99.84%	98.97%	99.73%	99.90%	98.68%
Zorflex FM10-700	98.77%	99.77%	99.68%	99.72%	99.76%	99.06%	99.49%	99.79%	98.77%
ACFC10V	98.42%	99.93%	99.97%	99.94%	99.84%	98.99%	99.98%	99.98%	95.05%
ACFC15V	95.89%	99.90%	99.93%	99.91%	99.83%	99.03%	99.92%	99.93%	92.69%
ACFC20V	94.57%	99.95%	99.95%	99.96%	99.93%	99.36%	99.93%	99.96%	91.56%
ACFC25V	92.93%	99.97%	99.91%	99.92%	99.91%	99.66%	99.80%	99.97%	88.79%
ACFC10H	92.67%	99.99%	99.97%	99.97%	99.95%	99.23%	99.87%	99.99%	88.37%
ACFC15H	91.55%	99.89%	99.88%	99.90%	99.95%	98.98%	99.72%	99.96%	88.39%
ACFC20H	93.60%	99.79%	99.77%	99.80%	99.88%	98.98%	99.52%	99.88%	93.49%
ACFC25H	91.78%	99.80%	99.78%	99.81%	99.88%	99.06%	99.44%	99.88%	89.93%
ACFC15A	96.94%	99.70%	99.90%	99.69%	99.36%	98.98%	99.75%	99.90%	96.94%
Max	99.12%	99.99%	99.97%	99.97%	99.95%	99.66%	99.98%	99.99%	
Min	91.55%	99.45%	99.68%	99.49%	99.36%	98.61%	99.44%		88.37%

Max and Min are the maximum and minimum r^2 value along each row or column. The Max/Max and Min/Min cells contain the maximum and minimum r^2 value for the entire table

The r^2 values can be misleading, though. It is enlightening to look at the graphs themselves and look for aberrations. The DR and Do & Do equations can be seen to have very significant overshoot near RH = 100%. This is occasionally experienced with the CIMF, and full CMMS as well. The DR and Do & Do equations also fail to capture the steepness of the S-shaped part of an adsorption curve. The LeVan equation sometimes returns a fit that is not monotonic, such as in ACFC10V. The Lagorsse equation does not fit very well on hydrophobic carbons such as ACFC20H, and for hydrophilic carbons such as ACFC15S often gives a desorption branch that is lower than the adsorption branch, which is an aphysical result. Several equations show strange jumps sometimes, such as Stoeckli and Do & Do and CIMF on eSpin near RH = 0%, and the DS4 on BPL.

It is important to remember that these correlations are for these specific carbons, and in fact most of the equations that perform poorly here usually performed well on the carbons examined in the papers in which these formulas were proposed.

11 Conclusions

There is a variety of equilibrium isotherm models in the literature. These models were compared over a diverse group of activated carbons. Although some of these models can fit the isotherms with an r^2 greater than 99%, none of these models are predictive. There are no isotherm models that model hysteresis with any reasonable degree of accuracy.

Observing water adsorption isotherms with hysteresis gives qualitative information about the chemistry and structure of the carbons. Carbons that are similar chemically have similarly-shaped isotherms, e.g., carbons from cellulosic materials.

Novoloid-based ACFC with hydrogen treatment is more hydrophobic and has a more idealized isotherm than any previously presented activated carbon. This material would be ideal for high-humidity adsorption applications.

Although no real material can be modeled as simply as a slit-shaped pore, the ACFC is an interesting material for the subject of further molecular adsorption simulations.

References

Barton, S.S., Evans, M.J.B., et al.: The adsorption of water vapor by porous carbon. Carbon **29**(8), 1099–1105 (1991)

Barton, S.S., Evans, M.J.B., et al.: An equation describing water vapour absorption on porous carbon. Carbon **30**(1), 123–124 (1992)

Brennan, J.K., Bandosz, T.J., et al.: Water in porous carbons. Colloids Surf. A: Physicochem. Eng. Aspects **187–188**, 539–568 (2001)

Cal, M.P., Rood, M.J., et al.: Removal of VOCs from humidified gas streams using activated carbon cloth. Gas Sep. Purif. **10**(2), 117–121 (1996)

Dimotakis, E., Cal, M., et al.: Water vapor adsorption on chemically treated activated carbon cloths. Chem. Mater. **7**(12), 2269–2272 (1995a)

Dimotakis, E.D., Cal, M.P., et al.: Chemically treated activated carbon cloths for removal of volatile organic carbons from gas streams: evidence for enhanced physical adsorption. Environ. Sci. Technol. **29**(7), 1876–1880 (1995b)

Do, D.D.: Adsorption Analysis: Equilibria and Kinetics. Imperial College Press, London (1998)

Do, D.D., Do, H.D.: A model for water adsorption in activated carbon. Carbon **38**(5), 767–773 (2000)

Doong, S.J., Yang, R.T.: Adsorption of mixtures of water vapor and hydrocarbons by activated carbon beds: Thermodynamic model for adsorption equilibrium and adsorber dynamics. AIChE Symposium Series: Adsorption and Ion Exchange **84**(259), 87–97 (1987)

Dubinin, M.M.: Water vapor adsorption and the microporous structures of carbonaceous adsorbents. Carbon **18**(5), 355–364 (1980)

Dubinin, M.M., Serpinsky, V.V.: Isotherm equation for water vapor adsorption by microporous carbonaceous adsorbents. Carbon **19**(5), 402–403 (1981)

Gauden, P.A.: Does the Dubinin–Serpinsky theory adequately describe water adsorption on adsorbents with high-energy centers? J. Colloid Interface Sci. **282**(2), 249–260 (2005)

Furmaniak, S., Gauden, P.A., et al.: Heterogeneous Do–Do model of water adsorption on carbons. J. Colloid Interface Sci. **290**(1), 1–13 (2005)

Hashisho, Z., Emamipour, H., et al.: Rapid response concentration-controlled desorption of activated carbon to dampen concentration fluctuations. Environ. Sci. Technol. **41**(5), 1753–1758 (2007)

Hayes, J.S., Jr.: Novoloid fibers. In: Kirk-Othmer: Encyclopedia of Chemical Technology, vol. 16, pp. 125–138. Wiley, New York (1981)

Huggahalli, M., Fair, J.R.: Prediction of equilibrium adsorption of water onto activated carbon. Ind. Eng. Chem. Res. **35**(6), 2071–2074 (1996)

Kimura, T., Kanoh, H., et al.: Cluster-associated filling of water in hydrophobic carbon micropores. J. Phys. Chem. B **108**(37), 14043–14048 (2004)

Lagorsse, S., Campo, M.C., et al.: Water adsorption on carbon molecular sieve membranes: experimental data and isotherm model. Carbon **43**(13), 2769–2779 (2005)

Qi, N., LeVan, M.D.: Adsorption equilibrium modeling for water on activated carbons. Carbon **43**(11), 2258–2263 (2005)

Li, L., Quinlivan, P.A., et al.: Effects of activated carbon surface chemistry and pore structure on the adsorption of organic contaminants from aqueous solution. Carbon **40**(12), 2085–2100 (2002)

Liu, J.C., Monson, P.A.: Does water condense in carbon pores? Langmuir **21**(22), 10219–10225 (2005)

Liu, J.C., Monson, P.A.: Monte Carlo simulation study of water adsorption in activated carbon. Ind. Eng. Chem. Res. **45**(16), 5649–5656 (2006)

Mahle, J.J.: An adsorption equilibrium model for Type 5 isotherms. Carbon **40**(15), 2753–2759 (2002)

Mangun, C.L., Benak, K.R., et al.: Oxidation of activated carbon fibers: effect on pore size, surface chemistry, and adsorption properties. Chem. Mater. **11**(12), 3476–3483 (1999)

Mays, T.J.: Active carbon fibers. In: Burchell, T.D. (ed.) Carbon Materials for Advanced Technologies, pp. 95–118. Pergamon, New York (1999)

Menendez, J.A., Phillips, J., et al.: On the modification and characterization of chemical surface properties of activated carbon: In the search of carbons with stable basic properties. Langmuir **12**(18), 4404–4410 (1996)

Ohba, T., Kaneko, K.: Cluster-associated filling of water molecules in slit-shaped graphitic nanopores. Mol. Phys. **105**(2), 139–145 (2007)

Petkovska, M., Mitrovic, M.: One-dimensional, nonadiabatic, microscopic model of electrothermal desorption process dynamics. Chem. Eng. Res. Des. **72**(A6), 713–722 (1994)

Qi, S., Hay, K.J., et al.: Isotherm equation for water vapor adsorption onto activated carbon. J. Environ. Eng. **124**(11), 1130–1134 (1998)

Rudisill, E.N., Hacskaylo, J.J., et al.: Coadsorption of hydrocarbons and water on BPL activated carbon. Ind. Eng. Chem. Res. **31**(4), 1122–1130 (1992)

Rutherford, S.W.: Application of cooperative multimolecular sorption theory for characterization of water adsorption equilibrium in carbon. Carbon **41**(3), 622–625 (2003)

Rutherford, S.W.: Modeling water adsorption in carbon micropores: study of water in carbon molecular sieves. Langmuir **22**(2), 702–708 (2006)

Stoeckli, F.: Water adsorption in activated carbons of various degrees of oxidation described by the Dubinin equation. Carbon **40**(6), 969–971 (2002)

Subrenat, A.S., Le Cloirec, P.A.: Volatile organic compound (VOC) removal by adsorption onto activated carbon fiber cloth and electrothermal desorption: an industrial application. Chem. Eng. Commun. **193**(4), 478–486 (2006)

Sullivan, P.D., Rood, M.J., et al.: Adsorption and electrothermal desorption of hazardous organic vapors. J. Environ. Eng. **127**(3), 217–223 (2001)

Sun, J., Chen, S., et al.: Correlating N_2 and CH_4 adsorption on microporous carbon using a new analytical model. Energy Fuels **12**(6), 1071–1078 (1998)

Talu, O., Francis, M.: Adsorption of associating water molecules in micropores and application to water on carbon. AIChE J. **42**(3), 809–819 (1996)

Vidal, E.X., Ramirez, D., et al.: Bench-scale and pilot-scale electrothermal-swing adsorption systems for the capture and recovery of hazardous air pollutants. In: Proceedings of the Air and Waste Management Association's Annual Conference and Exhibition, AWMA (2006)